Journal of Molecular Liquids 427 (2025) 127302

Contents lists available at ScienceDirect

Journal of Molecular Liquids

journal homepage: www.elsevier.com/locate/molliq

Influence of five protic and aprotic ionic liquids as anti-crystallization additives of water/lithium bromide on the solid–liquid equilibrium

David Latorre-Arca [a,c], M. Soledad Larrechi [b,c], Daniel Salavera [a,c,*], Alberto Coronas [a,c]

[a] Mechanical Engineering Dept, Universitat Rovira i Virgili, Tarragona, Spain
[b] Analytical and Organic Chemistry Dept, Universitat Rovira i Virgili, Tarragona, Spain
[c] Group of Research in Applied Thermal Engineering-CREVER, Universitat Rovira i Virgili, Tarragona, Spain

ARTICLE INFO

Keywords:
Ionic liquids
Solid–liquid equilibrium
Absorption refrigeration
Water/lithium bromide
Spectroscopic analysis

ABSTRACT

In this work, we study the influence of five ionic liquids (ILs) as anti-crystallization additives of water/lithium bromide (H_2O/LiBr) on the solubility of LiBr in H_2O. The selected ILs are ethylammonium nitrate [EA][NO_3], propylammonium nitrate [PA][NO_3], ethylammonium chloride [EA][Cl], 1-butyl-3-methylimidazolium bromide [Bmim][Br], and 1,3-dimethylimidazolium chloride [Dmim][Cl]. The solubility of LiBr in H_2O in the presence of these ILs was individually determined from (280–360) K at an IL/LiBr mole ratio around 0.0205, and at two additional IL/LiBr mole ratios in the case of ILs based on the imidazolium cation. A quantitative analysis of bulk water in H_2O/(LiBr+IL) mixtures was conducted using near-infrared spectroscopy and multivariate curve resolution. The amount of H_2O that does not interact with the solute (LiBr+IL), which is a measure of solute–solvent interactions, was estimated at 293.2 K, 313.2 K, and 333.2 K. In these solutions, in addition to the IL/LiBr mole ratio at 0.0205, two higher ratios were considered in the case of the mixture with [Dmim][Cl]. The results show that, on average, the selected ILs increase the solubility of LiBr in H_2O from 1.6 % to 5.7 %, and that this increment is more pronounced at lower temperatures. Protic ILs based on the ammonium cation enhance the solubility of LiBr more than aprotic ones based on the imidazolium cation, following the order: [EA][NO_3] ≈ [PA][NO_3] > [EA][Cl] ≈ [Bmim][Br] ≈ [Dmim][Cl]. Furthermore, the presence of ILs contributes to a higher amount of bulk water, which suggests that ILs interact with LiBr ions, competing with H_2O and favoring solubility. This interaction depends on both the chemical structure of the ILs, with protic ILs forming stronger bonds due to hydrogen bonding, and on the temperature, as the amount of bulk water decreases with an increase in temperature.

1. Introduction

Interest in absorption refrigeration systems and heat pumps has recently increased due to their unique advantages [1–4]. Unlike conventional refrigeration systems, which are electrical, absorption systems can be driven by waste heat or renewable heat sources, such as solar thermal energy or geothermal heat. The mixture of water and lithium bromide (H_2O/LiBr) is one of the most used working fluids in absorption cooling and heat pump systems [5]. Among other advantages, it stands out that this working pair does not contribute to global warming or the depletion of the ozone layer. However, the main disadvantage of the mixture is the risk of crystallization of LiBr, which limits the operating range of absorption systems.

In the selected applications, ionic liquids (ILs) have been proposed as absorbents in ammonia/IL [6–10] and H_2O/IL [11–16] mixtures, and as additives of LiBr in the H_2O/LiBr mixture to overcome the drawback of the crystallization of LiBr [17–24]. However, using ILs as absorbents in H_2O/IL mixtures results in a lower performance compared to H_2O/LiBr [16,18,22]. These ILs also face challenges related to transport properties, such as high viscosity [25] and low diffusion coefficients [26]. Nevertheless, it remains unclear whether ILs can be used successfully as anti-crystallization additives of LiBr as there are only limited studies providing experimental data (Table S1). This lack of data is mainly due to the large amount of time and money needed to experimentally determine the thermophysical properties of these mixtures.

The main objective of this work is to analyze the solubility of LiBr in H_2O in the presence of five ILs proposed as anti-crystallization additives from (280 to 360) K and anhydrous mass fraction of absorbent (LiBr+IL)

* Corresponding author at: Mechanical Engineering Dept, Universitat Rovira i Virgili, Tarragona, Spain.
E-mail address: daniel.salavera@urv.cat (D. Salavera).

https://doi.org/10.1016/j.molliq.2025.127302
Received 9 December 2024; Received in revised form 13 February 2025; Accepted 4 March 2025
Available online 7 March 2025

from 0.59 to 0.70. The selected ILs are ethylammonium nitrate ([EA][NO_3]), propylammonium nitrate ([PA][NO_3]), and ethylammonium chloride ([EA][Cl]), 1-butyl-3-methylimidazolium bromide ([Bmim][Br]), and 1,3-dimethylimidazolium chloride ([Dmim][Cl]). All of them have inorganic anions that interact with H_2O and relatively short alkyl chain lengths to avoid having a highly viscous working fluid with low mass diffusivity, which would impair its performance in the application of interest. The first three are protic ILs based on the ammonium cation and have not been used in any published work so far. The last two are aprotic ILs based on the imidazolium cation, which have already been used in the literature as additives of LiBr [27–29], extending the range in which the solubility is experimentally determined according to the application of interest. A comparative analysis of the amount of water that does not interact with the solute in the mixtures was carried out to interpret the influence of the ILs on the solubility of LiBr in H_2O. The IL/LiBr mole ratio was set to 0.0205 for all mixtures to avoid the aforementioned problems related to the transport properties of ILs, which could impair the performance of the working fluid in the application. The influence of the IL composition on the solubility was also analyzed with [Bmim][Br] and [Dmim][Cl] at two different IL/LiBr mole ratios in each case.

The comparative analysis of ion solvation requires selecting a criterion to evaluate the extension in which the ion solvation occurs in the presence of ILs. Since solute–solute, solute–solvent, and solvent–solvent interactions determine the macroscopic properties of electrolyte solutions [30–32], different approaches have been used to research them. Computational studies are commonly used to analyze the solvation of salts in solution. Examples in the literature include Molecular Dynamics simulations to study the interactions between electrolytes and ILs [33–35], or ILs and H_2O [36–40]. Other approaches are based on the mass action law, ion solvation, and ion pairing phenomena [41–45].

While ion solvation studies contribute to understanding the behavior of electrolyte solutions, this is not the objective of the present work. Instead, we have used infrared spectroscopy coupled with the multivariate curve resolution methods based on alternating least squares to calculate the amount of bulk water in the solutions, which measures the global interaction between the solvent and the solute [9,10,46–49]. This approach has been used to determine the amount of water that does not interact with the solute (LiBr or LiBr+IL). For this purpose, the near-infrared spectra of at least 12 solutions prepared with anhydrous solute mole fractions varying from 0 to 0.22 were acquired at 293.2 K, 313.2 K, and 333.2 K. The IL/LiBr mole ratio was 0.0205 in all H_2O/

Table 1
Ionic liquids used as additives of H_2O/LiBr.

Compound, abbreviation, and CAS number	Supplier and mass purity (%)	Cation	Anion	M(g·mol^{-1})
Ethylammonium nitrate ([EA][NO_3]) 22113-86-6	IOLITEC (> 97)	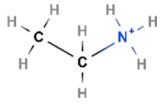	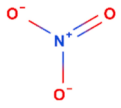	108.11
Propylammonium nitrate ([PA][NO_3]) 22113-88-8	IOLITEC (> 97)	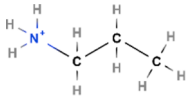	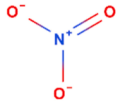	122.12
Ethylammonium chloride ([EA][Cl]) 557-66-4	Sigma-Aldrich(> 99.3)	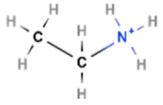	Cl^-	81.545
1-butyl-3-methylimidazolium bromide ([Bmim][Br]) 85100-77-2	IOLITEC (> 99)	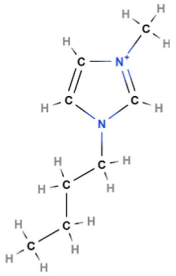	Br^-	219.12
1,3-dimethylimidazolium chloride ([Dmim][Cl]) 79917-88-7	Angene (> 97)	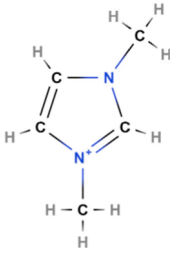	Cl^-	132.59

(LiBr+IL) solutions. The H_2O/(LiBr+[Dmim][Cl]) mixture was also analyzed at IL/LiBr mole ratios of 0.0418 and 0.0648.

2. Experimental section and data analysis

2.1. Solid-liquid phase equilibrium

H_2O/(LiBr+IL) samples were prepared with anhydrous mass fractions of absorbent (LiBr+IL) from 0.59 to 0.70 to determine the solid–liquid equilibrium (SLE), which corresponds to equilibrium temperatures between 280 K and 360 K. The IL/LiBr mole ratio was set to 0.0205 for all the mixtures (Tables 2–5), and two additional ratios were considered for the imidazolium-based ILs to analyze the influence of their composition on the solubility of LiBr.

The abovementioned solutions were prepared with LiBr (CAS No: 7550-35-8) purchased from Sigma-Aldrich (mass purity greater than 99 %), and Millipore H_2O with a resistivity of 18.2 MΩ·cm. Information regarding the selected ILs is shown in Table 1. Before use, LiBr, [Bmim][Br], [Dmim][Cl], and [EA][Cl] were dried in an oven at 373 K for 24 h. [EA][NO_3] and [PA][NO_3], which are liquid at room temperature, were subjected to vacuum (3 kPa), with stirring and heating at 373 K for 24 h.

The equilibrium temperature was determined with a Pt-100 temperature probe connected to a F250 Mk II Precision Thermometer (±0.01 K) by means of the visual-polythermal-synthetic method, in which the phase change of a solution with known composition is observed with the naked eye. The starting point is a concentrated solution with visible precipitate, to which the temperature is manually increased by 0.1 K every 15 min while stirring until the solid phase is no longer observed. Further information regarding the method and the equipment can be found elsewhere [5,49,50].

H_2O/(LiBr+IL) solutions used to determine the SLE were prepared by weight with a Mettler Toledo ME403 balance (resolution = 0.001 g). First, a known mass of LiBr was introduced into the equilibrium cell. Then, Millipore H_2O was added to achieve a solution with an anhydrous mass fraction of LiBr equal to 0.69. Subsequently, the stirrer was added, and the temperature of the thermostatic bath was set to 373 K until the crystals were dissolved. The required mass of IL was then added to reach the desired IL/LiBr mole ratio, and the saturation temperature of that solution was determined. Finally, known amounts of H_2O were added to dilute the initial solution and obtain the solubility curve. The experiments were conducted from (280 to 360) K.

The SLE of H_2O/(LiBr+IL) mixtures was analyzed considering the anhydrous absorbent composition, as is commonly done in the literature [27,28,49,51–53]. However, interpreting the results from this point of view is challenging, since the greater solubility of the absorbent in the presence of ILs is related both to the interactions between ions and molecules in the mixture and the replacement of part of the LiBr by IL. Therefore, the mole fraction ratio between anhydrous (prepared) LiBr and H_2O (x_{LiBr}/x_{H_2O}) was compared to that of H_2O/LiBr in relative terms (Eq. (1)) over the entire temperature range. To the best of our knowledge, this constitutes a novel way of interpreting the influence of additives on the properties of the working fluid. The main advantage is that it makes it possible to analyze the influence of the additive independently of the nature of the additive and its composition in the mixture. In addition, the SLE is also interpreted depending on the chemical structure of the ILs.

$$\Delta x/x(\%) = 100 \cdot \frac{\left(\frac{x_{LiBr}}{x_{H_2O}}\right)_{H_2O/(LiBr+IL)} - \left(\frac{x_{LiBr}}{x_{H_2O}}\right)_{H_2O/LiBr}}{\left(\frac{x_{LiBr}}{x_{H_2O}}\right)_{H_2O/LiBr}} \quad (1)$$

2.2. Near-infrared spectroscopy and MCR-ALS resolution

H_2O/(LiBr+IL) solutions used to estimate the *BW* in solution were prepared with anhydrous mole fractions of solute (either LiBr or LiBr+IL) ranging from 0 to 0.22 and with an IL/LiBr mole ratio of 0.0205. The influence of the IL composition was analyzed in the case of H_2O/(LiBr+[Dmim][Cl]) solutions at IL/LiBr mole ratios equal to 0.0418 and 0.0648. Information regarding the reagents is detailed in the previous section of this work. These electrolyte solutions were prepared by weight using a Mettler Toledo AE 260 Delta Range analytical balance (resolution = 0.0001 g) from an initial H_2O/LiBr solution with a LiBr mass fraction equal to 0.58. Then, the required amount of IL was added, and further dilutions were achieved by adding pure H_2O to a known mass of the initial solution.

The spectra of H_2O/(LiBr+IL) solutions were acquired from 800 nm to 1060 nm at 293.2 K, 313.2 K, and 333.2 K with a contact thermometer model ETS-D5 (±0.1 K) and a UV–visible 8453 Agilent spectrophotometer equipped with optical fibers. As detailed in a previous work [48], the spectra of H_2O/LiBr solutions were obtained between 900 nm and 1060 nm with an Ocean Optics UV–vis-NIR (Maya 2000 pro). In both cases, the absorbance mode was used, and 100 % of the transmittance was established with a 1 cm path-length quartz cell filled with air before the sample analysis at each temperature. The cell was filled with 1.5 mL of each sample to acquire its spectrum. The temperature of the samples was measured and kept constant by a H_2O thermostatic bath in which the cell was immersed. The spectra were sequentially acquired from pure H_2O to the highest solute composition.

A brief explanation of the bulk water estimation is given here. Further information is available in the authors' previous works [10,39,46–49]. The spectra of each mixture were arranged in separate data matrices (**D**) at each temperature using Matlab [54]. The Multivariate Curve Resolution method based on Alternating Least Squares (MCR-ALS) was used to decompose each **D** matrix into the product of concentration (**C**) and spectral (**S**) profiles of the different chemical species according to Eq. (2) [55], where **E** is the residual matrix that the model does not explain. This process was carried out in various steps using the toolbox developed by Jaumot et al. [56]. First, the number of factors (*f*) in each mixture, which represents the different chemical environments in which H_2O is present, was determined by the explained variance obtained from the singular value decomposition of the **D** matrices. Then, an initial estimation of either the concentration profile or the spectral profile is required. In this work, the concentration profile of the species in each mixture was estimated with evolving factor analysis (EFA) [57]. Finally, this initial estimation was optimized by solving Eq. (2) iteratively using the Alternating Least Squares (ALS) method [58] until the difference in the residual of two consecutive iterations between the obtained solution and the experimental spectra was lower than the tolerance, which was set to 0.01. In this optimization process, the restrictions used were non-negativity of spectra and concentration profiles, unimodality of concentration profiles, and normalization of the spectra.

$$\mathbf{D} = \mathbf{C} \cdot \mathbf{S}^{\mathbf{T}} + \mathbf{E} \quad (2)$$

Finally, the mole fraction of H_2O that does not participate in the hydration of the solute (*BW*), preserving the structural properties of pure H_2O, was estimated for all solutions from the concentration profile of the chemical species that corresponds to bulk water. This mole fraction, expressed in percentage, was calculated as the ratio between the recovered moles of H_2O in each solution to the moles of H_2O in the first solution, which is pure H_2O (Eq. (3)).

$$BW(\%) = 100 \cdot \frac{n_{H_2O,recovered}}{n_{H_2O,pure}} \quad (3)$$

3. Results and discussion

3.1. Solid–liquid phase equilibrium of H_2O/(LiBr+IL) mixtures

Tables 2 and 3 show the saturation temperature and the absorbent (LiBr or LiBr+IL) mass fraction of the different H_2O/(LiBr+IL) mixtures.

Table 2
Solid-liquid equilibrium data of H_2O/(LiBr+IL) mixtures with protic ILs. w_{abs}: anhydrous mass fraction of absorbent; T: temperature; x_{IL}/x_{LiBr}: mole fraction ratio between IL and LiBr.

H_2O/(LiBr+[EA][NO_3]) x_{IL}/x_{LiBr} = 0.0207				H_2O/(LiBr+[PA][NO_3]) x_{IL}/x_{LiBr} = 0.0206				H_2O/(LiBr+[EA][Cl]) x_{IL}/x_{LiBr} = 0.0205			
w_{abs}	T(K)	w_{abs}	T(K)	w_{abs}	T(K)	w_{abs}	T(K)	w_{abs}	T(K)	w_{abs}	T(K)
0.696	362.6	0.647	310.0	0.693	359.5	0.663	319.3	0.695	366.3	0.643	310.2
0.692	358.7	0.641	308.0	0.689	355.0	0.661	314.8	0.692	362.9	0.638	308.1
0.689	354.6	0.636	305.7	0.686	351.1	0.658	313.5	0.688	358.9	0.631	304.9
0.685	350.4	0.631	303.4	0.682	346.4	0.654	312.5	0.685	354.8	0.624	301.7
0.681	345.4	0.626	300.8	0.679	341.8	0.650	311.3	0.681	350.4	0.618	298.4
0.677	340.3	0.622	298.2	0.675	337.2	0.646	309.6	0.677	345.8	0.613	295.1
0.673	335.0	0.617	295.5	0.673	333.3	0.642	308.0	0.674	341.0	0.607	291.5
0.670	330.6	0.614	293.4	0.669	328.5	0.638	306.3	0.670	336.3	0.603	288.8
0.667	325.9	0.610	290.9	0.666	323.9	0.633	304.3	0.666	331.0	0.599	285.8
0.664	321.2	0.606	288.5	0.663	319.3			0.663	325.6	0.595	282.9
0.661	316.3	0.603	285.8	0.661	314.8			0.659	320.2	0.592	279.9
0.658	314.1	0.599	282.6	0.658	313.5			0.656	314.6		
0.656	313.2	0.595	279.3	0.654	312.5			0.652	313.4		
0.652	312.1			0.650	311.3			0.649	312.0		

$U(T)$ = 0.1 K; $U(w_{abs})$ = 0.001.

To analyze the influence of ILs on solubility, Fig. 1 shows the solubility curves of the H_2O/(LiBr+IL) mixtures at $x_{IL}/x_{LiBr} \approx 0.0205$ along with the solubility curve of H_2O/LiBr obtained by Salavera et al. [50], who used the same experimental device as in this work. There is a trend in the change in the solubility curve of all mixtures between 311 K and 315 K, corresponding to a change in the amount of H_2O molecules with which LiBr precipitates from dihydrate to monohydrate [28,51,59]. In H_2O/(LiBr+IL) mixtures, although ILs could be present in the precipitate, they do not affect the amount of H_2O molecules in the solid phase compared to that of H_2O/LiBr [28,51]. It is observed that a higher amount of absorbent can be dissolved in H_2O in the presence of ILs over the entire temperature range, which is in agreement with the literature [27,28,49,51–53].

Fig. 2 shows that the higher the amount of IL in the absorbent, the higher the amount of absorbent that can be dissolved in H_2O at the same temperature. However, the increase in solubility is not directly proportional to the IL composition. This behavior was attributed to the interactions between LiBr and ILs [28,51].

SLE results have also been analyzed from the point of view of the anhydrous LiBr/H_2O mole ratio according to Eq. (1). Fig. 3 shows the relative x_{LiBr}/x_{H_2O} increment of the mixtures with the additive with respect to H_2O/LiBr. It can be seen that the values are always positive and range from 0.2 % to 8.7 %, which evidences that the solubility of LiBr in H_2O is higher in the presence of the selected ILs and compositions. Thus, ILs act as anti-crystallization additives, preventing the formation of solid phase in conditions where LiBr would otherwise precipitate, as described by the general chemical equilibrium condition: LiBr·n·H_2O (s) ↔ LiBr (L) + n·H_2O (L) [28]. Moreover, the relative increase in x_{LiBr}/x_{H_2O} is influenced by temperature, which is expected given that the structural conformations of ILs and chemical species in the medium depend strongly on temperature [26]. The higher values between 311 K and 315 K correspond to the change in the amount of H_2O molecules in the solid phase.

Table 4 shows the average relative increase in the x_{LiBr}/x_{H_2O} ratio as a function of temperature and IL composition for each mixture. These results show that the increase in solubility depends on the nature of the IL, its composition in the mixture, and the temperature.

It is striking to observe an increase in the solubility of LiBr in H_2O in the mixtures with [Bmim][Br], where the IL and LiBr have the same anion. In agreement with Méndez-Morales et al. [33], who discussed the interactions between lithium nitrate and ethylammonium nitrate, the positive values found for our mixtures suggest strong interactions between the cations of LiBr and ILs. A comparison of their significance can be seen in Fig. 3 at $x_{IL}/x_{LiBr} \approx 0.0205$, where ILs based on the ammonium cation increase the solubility of LiBr in H_2O slightly more than ILs based on the imidazolium cation according to the following order: [EA][NO_3] ≈ [PA][NO_3] > [EA][Cl] ≈ [Bmim][Br] ≈ [Dmim][Cl].

Regarding the influence of the chemical structure of the ILs, it is observed that, on one hand, the difference between the cations of [EA][NO_3] and [PA][NO_3] lies only in the size of the alkyl chain. Although the increase in the x_{LiBr}/x_{H_2O} ratio is slightly higher with the former IL than with the latter, the differences are not significant for the IL/LiBr ratios used in this work. Nevertheless, it is believed that the propyl group, which is larger than the ethyl group, is associated with a higher hydrophobicity, which is not beneficial for dissolving more LiBr in H_2O [28,51].

On the other hand, the difference between the cation of [EA][Cl] and [Dmim][Cl] lies simultaneously in the cation base (ammonium vs. imidazolium) and in the length of the alkyl chain. However, the difference in the increase in solubility of LiBr in H_2O between these two additives cannot be interpreted solely based on these results, as this requires information regarding interactions in the solution.

3.2. Quantitative analysis of bulk water

Detailed information regarding pre-treated spectra, composition, and *BW* calculated by MCR-ALS in H_2O/LiBr and H_2O/(LiBr+IL) solutions is reported in Figs. S1–S17 and Tables S2-S5 in the Supplementary Information.

As an example of the results found to estimate the *BW* in all the mixtures analyzed, we discuss here the results obtained for the H_2O/(LiBr+[Dmim][Cl]) solutions at x_{IL}/x_{LiBr} = 0.0648. Fig. 4 shows the spectra of four solutions of this mixture, where the characteristic absorption band of the stretching vibration of the –OH group around 971 nm decreases with solute composition and shifts towards longer wavelengths.

An estimation of the number of different chemical environments in which H_2O molecules coexist in the solutions was obtained with the MCR-ALS of the NIR spectra. In all cases, two factors, representatives of them, were required to preserve almost the entire variability of individual **D** matrices. In all the considered mixtures, the explained variance and the lack of fit of the MCR-ALS solutions ranged from 99.89 % to 99.98 % and from 1.29 % to 3.29 %, respectively.

Fig. 5 shows the MCR-ALS results of the decomposition of the data matrix for the H_2O/(LiBr+[Dmim][Cl]) solutions at 293.2 K with x_{IL}/x_{LiBr} = 0.0648. The correlation coefficient between the experimental spectrum of pure H_2O and the recovered spectrum with the maximum value obtained at 976 nm is 0.9982. For this reason, this chemical environment has been considered representative of bulk water in these solutions. The maximum absorbance of the other recovered spectrum is

Table 3
Solid-liquid equilibrium data of H_2O/(LiBr+IL) mixtures with aprotic ILs. w_{abs}: anhydrous mass fraction of absorbent; T: temperature; x_{IL}/x_{LiBr}: mole fraction ratio between IL and LiBr.

H_2O/(LiBr+[Bmim][Br])												H_2O/(LiBr+[Dmim][Cl])											
x_{IL}/x_{LiBr} = 0.0121			x_{IL}/x_{LiBr} = 0.0209			x_{IL}/x_{LiBr} = 0.0301			x_{IL}/x_{LiBr} = 0.0205			x_{IL}/x_{LiBr} = 0.0426			x_{IL}/x_{LiBr} = 0.0491							
w_{abs}	T (K)	w_{abs}	T (K)	w_{abs}	T (K)	w_{abs}	T (K)	w_{abs}	T (K)	w_{abs}	T (K)	w_{abs}	T (K)	w_{abs}	T (K)	w_{abs}	T (K)	w_{abs}	T (K)	w_{abs}	T (K)	w_{abs}	T (K)
0.696	366.5	0.646	312.1	0.701	365.0	0.658	313.8	0.706	366.0	0.663	313.7	0.697	366.6	0.648	311.3	0.694	350.3	0.705	361.4	0.660	309.3		
0.692	362.8	0.639	309.2	0.698	361.7	0.655	312.6	0.703	362.7	0.659	312.4	0.693	362.6	0.644	309.9	0.680	332.7	0.702	357.5	0.654	307.1		
0.689	359.2	0.632	305.9	0.695	357.8	0.649	310.3	0.700	358.9	0.653	310.2	0.690	358.6	0.639	307.7	0.672	322.3	0.698	353.0	0.647	304.5		
0.685	354.6	0.625	302.9	0.691	353.7	0.643	307.7	0.696	354.8	0.646	307.1	0.686	353.8	0.631	304.4	0.665	311.8	0.693	348.3	0.641	301.5		
0.681	349.8	0.619	299.5	0.688	349.6	0.637	304.7	0.692	350.2	0.638	303.5	0.682	348.9	0.624	300.9	0.659	309.9	0.689	343.2	0.635	298.4		
0.677	344.6	0.612	295.1	0.684	345.2	0.630	301.5	0.689	345.7	0.631	299.5	0.678	344.5	0.617	296.8	0.652	307.3	0.685	337.6	0.628	294.9		
0.673	339.3	0.608	292.7	0.681	340.8	0.623	297.3	0.685	340.9	0.624	295.3	0.674	339.2	0.610	292.1	0.643	303.6	0.681	332.0	0.622	291.2		
0.669	333.7	0.603	289.1	0.678	336.0	0.617	293.3	0.681	336.0	0.618	291.0	0.670	333.7	0.603	287.2	0.635	299.7	0.678	328.5	0.616	287.3		
0.665	327.7	0.598	285.2	0.674	331.3	0.610	288.3	0.678	330.7	0.611	286.0	0.666	328.5	0.598	283.3	0.627	295.4	0.675	324.3	0.611	283.2		
0.661	321.7	0.593	281.0	0.671	326.5	0.605	284.4	0.674	325.0	0.604	280.6	0.662	322.7	0.593	279.5	0.620	290.9	0.672	319.5	0.607	279.7		
0.658	316.4			0.668	321.2	0.599	280.1	0.671	319.4	0.598	275.4	0.659	317.0			0.614	286.9	0.669	314.5				
0.654	315.0			0.665	315.9			0.669	315.8			0.655	313.6			0.607	281.5	0.666	311.2				
0.651	313.5			0.662	314.7			0.667	314.9			0.652	312.5			0.599	275.3	0.663	310.2				

$U(T)$ = 0.1 K; $U(w_{abs})$ = 0.001.

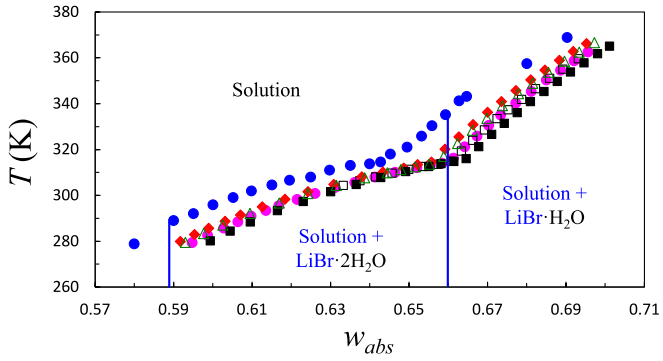

Fig. 1. Saturation temperature in relation to the mass fraction of the absorbent for the H_2O/LiBr and H_2O/(LiBr+IL) mixtures with $x_{IL}/x_{LiBr} \approx 0.0205$. ●: H_2O/LiBr [50]; |: Isocomposition lines [59]; ●: H_2O/(LiBr+[EA][NO_3]): □: H_2O/(LiBr+[PA][NO_3]); ◆: H_2O/(LiBr+[EA][Cl]); ■: H_2O/(LiBr+[Bmim][Br]); △: H_2O/(LiBr+[Dmim][Cl]).

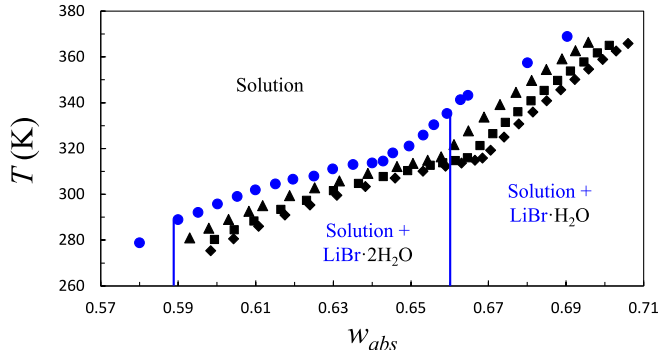

Fig. 2. Saturation temperature in relation to the mass fraction of the absorbent for the H_2O/LiBr and H_2O/(LiBr+[Bmim][Br]) mixtures. ●: H_2O/LiBr [50]; |: Isocomposition lines [59]; ▲: H_2O/(LiBr+[Bmim][Br]) with x_{IL}/x_{LiBr} = 0.0121; ■: H_2O/(LiBr+[Bmim][Br]) with x_{IL}/x_{LiBr} = 0.0209; ◆: H_2O/(LiBr+[Bmim][Br]) with x_{IL}/x_{LiBr} = 0.0301.

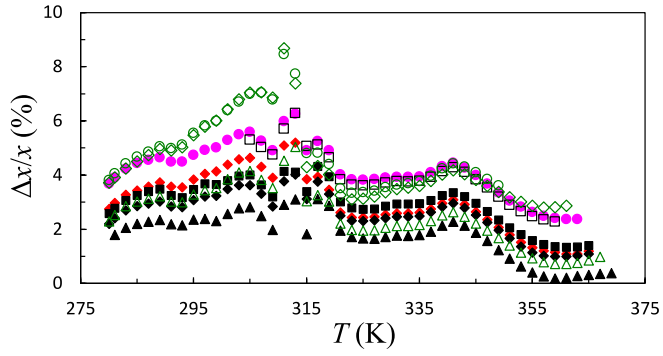

Fig. 3. The relative difference in the LiBr/H_2O mole ratio between the H_2O/(LiBr+IL) mixtures and H_2O/LiBr in relation to temperature. ●: H_2O/(LiBr+[EA][NO_3]); □: H_2O/(LiBr+[PA][NO_3]); ◆: H_2O/(LiBr+[EA][Cl]); ▲: H_2O/(LiBr+[Bmim][Br]) with x_{IL}/x_{LiBr} = 0.0121; ■: H_2O/(LiBr+[Bmim][Br]) with x_{IL}/x_{LiBr} = 0.0209; ◆: H_2O/(LiBr+[Bmim][Br]) with x_{IL}/x_{LiBr} = 0.0301; △: H_2O/(LiBr+[Dmim][Cl]) with x_{IL}/x_{LiBr} = 0.0205; ○: H_2O/(LiBr+[Dmim][Cl]) with x_{IL}/x_{LiBr} = 0.0426; ◇: H_2O/(LiBr+[Dmim][Cl]) with x_{IL}/x_{LiBr} = 0.0491.

at a longer wavelength (986 nm), as was observed in both H_2O/IL [47,48] and H_2O/salt [46,48,49] mixtures. For this reason, it has been considered representative of H_2O molecules hydrating the ions and is labeled as "associated water". As the solute composition increases, the concentration of bulk water decreases even in very dilute solutions,

Table 4
Summary of the average relative increase in x_{LiBr}/x_{H_2O} as a function of the ionic liquid, the IL/LiBr mole ratio, and temperature.

IL	x_{IL}/x_{LiBr}	$\Delta x/x$(%)	
		(280–311) K	(311–365) K
[EA][NO_3]	0.0207	4.8	3.9
[PA][NO_3]	0.0206	4.6*	3.8*
[EA][Cl]	0.0205	3.9	2.5
[Bmim][Br]	0.0121	2.3	1.6
	0.0209	3.5	2.7
	0.0301	3.1	2.3
[Dmim][Cl]	0.0205	3.4	2.0
	0.0426	5.7	4.3*
	0.0491	5.7	3.8

* Data not available over the entire temperature range considered.

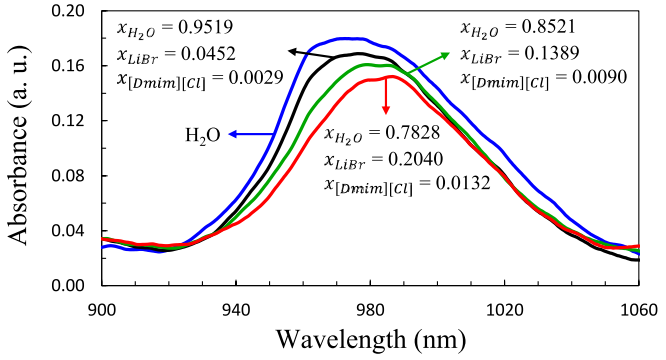

Fig. 4. Pre-treated NIR spectra of selected H_2O/(LiBr+[Dmim][Cl]) solutions with x_{IL}/x_{LiBr} = 0.0648 and 293.2 K.

which means that H_2O is hydrating the ions, while that of associated water increases. Similar information was also obtained for the other analyzed mixtures.

According to the Beer-Lambert law, the arbitrary values recovered through MCR-ALS are directly proportional to the real mole concentration of bulk water in solution. Under this premise, the *BW* values in each solution were determined by normalizing the bulk water concentrations, presented in Fig. 5 a), with respect to the recovered concentration of pure H_2O (0.186 mol·L^{-1}), which is the first solution included in the spectral data matrix. The aforementioned arbitrary concentration value represents the concentration of pure H_2O at 293.2 K (55.4 mol·L^{-1}). Then, for each solution, the recovered *BW* value was obtained by dividing the recovered moles of H_2O by the recovered moles of H_2O in pure water according to Eq. (3). *BW* results for other mixtures are reported in Tables S2–S4 in Supplementary Information.

Fig. 6 shows the *BW* values in relation to the mole fraction ratio between LiBr and H_2O for the analyzed mixtures at 293.2 K. All H_2O/(LiBr+IL) mixtures have more bulk water than H_2O/LiBr over the entire composition range, which is directly related to the increased solubility of LiBr in the presence of ILs. This suggests that interactions between LiBr and ILs compete with H_2O and LiBr interactions in H_2O/(LiBr+IL) mixtures, favoring the formation of large ionic aggregates over the entire composition range [60,61]. This interpretation agrees with the one reported previously by the authors for H_2O/(LiBr+[Dmim][Cl]) solutions at higher x_{IL}/x_{LiBr} ratios [48].

At $x_{IL}/x_{LiBr} \approx 0.0205$, H_2O/(LiBr+IL) solutions with ILs based on the ammonium cation have a greater *BW* than those with ILs based on the imidazolium cation, following the general order: [EA][Cl] > [EA][NO_3] ≈ [PA][NO_3] ≈ [Dmim][Cl] ≈ [Bmim][Br]. This could be explained by the formation of complex structures through hydrogen bonding by the former ILs [38–40].

Fig. 7 shows the *BW* of H_2O/LiBr and H_2O/(LiBr+IL) solutions as a function of the LiBr/H_2O mole fraction ratio at 313.2 K and 333.2 K. It is observed that the *BW* increases with increasing temperature over the entire composition range. This behavior can be attributed to the increase in the kinetic energy of the molecules with temperature, which causes the intermolecular interactions of the chemical species in the solutions to decrease [30].

The comparative analysis of Fig. 7 reveals that, regardless of temperature, the *BW* in the H_2O/(LiBr+[Bmim][Br]) mixture is lower than that in mixtures with ILs based on the ammonium cation. At 333.2 K, it is observed that the mixture with [Bmim][Br] has slightly lower *BW* values than H_2O/LiBr, which could indicate that LiBr has a greater H_2O absorption capacity in the presence of this additive.

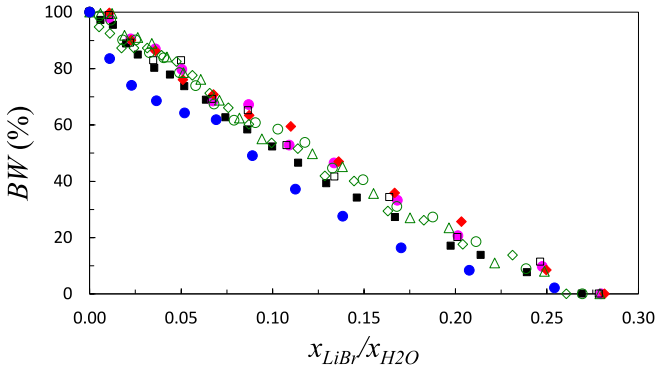

Fig. 6. *BW* of H_2O/LiBr and H_2O/(LiBr+IL) solutions against the mole fraction ratio between LiBr and H_2O at 293.2 K. ●: H_2O/LiBr [48]; △: H_2O/(LiBr+[Dmim][Cl]) with x_{IL}/x_{LiBr} = 0.0202; ○: H_2O/(LiBr+[Dmim][Cl]) with x_{IL}/x_{LiBr} = 0.0418; ◇: H_2O/(LiBr+[Dmim][Cl]) with x_{IL}/x_{LiBr} = 0.0648; ●: H_2O/(LiBr+[EA][NO_3]) with x_{IL}/x_{LiBr} = 0.0205; □: H_2O/(LiBr+[PA][NO_3]) with x_{IL}/x_{LiBr} = 0.0205; ◆: H_2O/(LiBr+[EA][Cl]) with x_{IL}/x_{LiBr} = 0.0205; ◆: H_2O/(LiBr+[Bmim][Br]) with x_{IL}/x_{LiBr} = 0.0208.

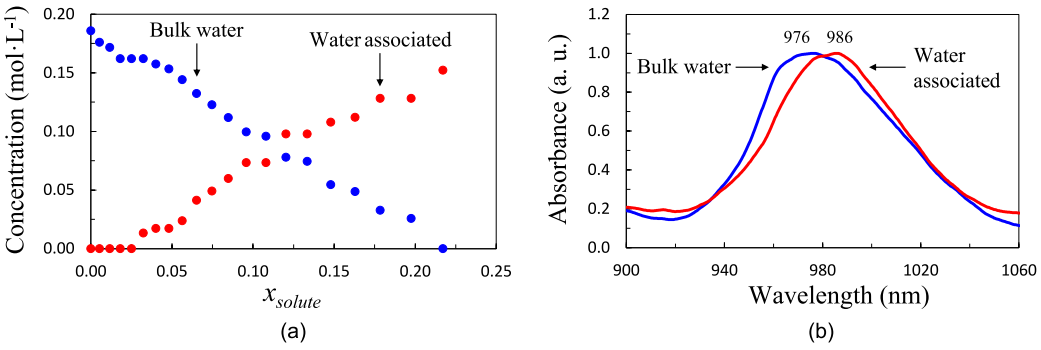

Fig. 5. Concentration (a) and spectral (b) profiles recovered by MCR-ALS for the H_2O/(LiBr+[Dmim][Cl]) solutions with x_{IL}/x_{LiBr} = 0.0648 at 293.2 K. Blue: bulk water. Red: associated water.

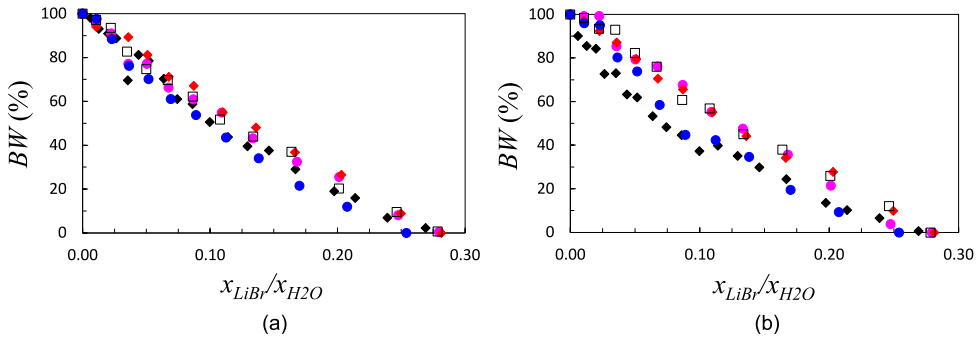

Fig. 7. *BW* of H_2O/LiBr and H_2O/(LiBr+IL) solutions against the mole fraction ratio between LiBr and H_2O at (a) 313.2 K and (b) 333.2 K. ●: H_2O/LiBr; ●: H_2O/(LiBr+[EA][NO_3]) with x_{IL}/x_{LiBr} = 0.0205; □: H_2O/(LiBr+[PA][NO_3]) with x_{IL}/x_{LiBr} = 0.0205; ◆: H_2O/(LiBr+[EA][Cl]) with x_{IL}/x_{LiBr} = 0.0205; ◆: H_2O/(LiBr+[Bmim][Br]) with x_{IL}/x_{LiBr} = 0.0208.

To provide information on the influence of temperature, Table 5 shows the average *BW* difference (Δ*BW*) of H_2O/(LiBr+IL) mixtures with respect to H_2O/LiBr over the entire composition range. At 313.2 K and 333.2 K, the Δ*BW* values are ordered as follows depending on the IL: [EA][Cl] ≈ [PA][NO_3] ≈ [EA][NO_3] > [Bmim][Br]. Although these findings cannot be interpreted based on NIR + MCR-ALS results alone, they could be analyzed using computational methods that allow further study of the interactions between ions in these solutions [39,48].

Before the conclusions, it is interesting to relate the results discussed throughout this paper. The higher bulk water values in the H_2O/(LiBr+IL) solutions over the entire temperature and composition range would justify that more LiBr can be dissolved in H_2O as the presence of the selected ILs delays its crystallization. This result evidences that there are interactions between LiBr and ILs, which has already been discussed in previous works with [Dmim][Cl] [19,20,48].

The comparative analysis at x_{IL}/x_{LiBr} ≈ 0.0205 shows that H_2O/(LiBr+IL) mixtures with protic ILs ([EA][NO_3], [PA][NO_3], and [EA][Cl]) exhibit larger average bulk water differences (Table 5) and increments of LiBr solubility in H_2O (Table 4) than the mixtures with aprotic ILs ([Bmim][Br] and [Dmim][Cl]). These results could indicate a higher degree of interaction between LiBr and protic ILs as a consequence of the smaller number of carbon atoms in ethylammonium ($[C_2H_5NH_3]^+$) and propylammonium ($[C_3H_7NH_3]^+$) cations than in 1,3-dimethylimidazolium ($[C_5H_9N_2]^+$) and 1-butyl-3-methylimidazolium ($[C_8H_{15}N_2]^+$) cations.

Although the average *BW* difference of H_2O/(LiBr+[Dmim][Cl]) solutions with respect to H_2O/LiBr remains relatively constant when working at x_{IL}/x_{LiBr} = 0.0202, 0.0418, and 0.0648 (Table 5), the increase in solubility of LiBr in H_2O is remarkable when the IL/LiBr mole ratio is increased from 0.0205 to 0.0426. This suggests that there are significant changes in solute–solute and solute–solvent interactions when there is a higher ionic liquid composition in the mixture.

4. Conclusions

The solubility of LiBr in H_2O increases in the presence of the selected additives at all IL/LiBr ratios considered, effectively increasing the operation range of absorption refrigeration and heat pump systems. The average relative increase in solubility of LiBr in H_2O ranges from 1.6 % to 5.7 % and is higher from (280 to 311) K than from (311 to 365) K in all cases. At x_{IL}/x_{LiBr} ≈ 0.0205, protic ILs increase the solubility of LiBr more than aprotic ILs, following the order: [EA][NO_3] ≈ [PA][NO_3] > [EA][Cl] ≈ [Bmim][Br] ≈ [Dmim][Cl]. This finding is attributed to the competitive reaction between the IL and H_2O for Li^+ and Br^- ions. However, there is a limit to the increase in solubility depending on the composition of the IL in the mixture. In the case of the mixture with [Bmim][Br], where the IL and LiBr have a common ion, the higher solubility of LiBr in H_2O suggests that there is an interaction between the lithium cation and the cation of the IL that cancels the effect of the common ion.

Table 5
Average bulk water difference (Δ*BW*) between H_2O/(LiBr+IL) and H_2O/LiBr mixtures.

Mixture	x_{IL}/x_{LiBr}	Δ*BW*(%)		
		293.2 K	313.2 K	333.2 K
H_2O/(LiBr+[Dmim][Cl])	0.0202	11.7	–	–
	0.0418	12.1	–	–
	0.0648	10.7	–	–
H_2O/(LiBr+[EA][NO_3])	0.0205	13.0	6.9	10.0
H_2O/(LiBr+[PA][NO_3])	0.0205	12.2	7.0	11.4
H_2O/(LiBr+[EA][Cl])	0.0205	14.6	10.2	10.7
H_2O/(LiBr+[Bmim][Br])	0.0208	7.9	3.6	−2.6

The estimation of bulk water in H_2O/LiBr and H_2O/(LiBr+IL) shows that there is more H_2O preserving the molecular structure of pure H_2O in the presence of all ILs at 293.2 K, 313.2 K, and 333.2 K, except for the mixture with [Bmim][Br] at 333.2 K. The higher *BW* in the mixtures with additives than in H_2O/LiBr suggests that ILs compete with H_2O for the Li^+ and Br^- ions in the solution, allowing more LiBr to dissolve. The *BW* in mixtures with ILs based on the ammonium cation is higher than in mixtures with ILs based on the imidazolium cation. There are no significant differences between the *BW* obtained at 293.2 K, 313.2 K, and 333.2 K, which decreases according to the following general order: H_2O/(LiBr+[EA][Cl]) > H_2O/(LiBr+[EA][NO_3]) ≈ H_2O/(LiBr+[PA][NO_3]) ≈ H_2O/(LiBr+[Dmim][Cl]) > H_2O/(LiBr+[Bmim][Br]).

CRediT authorship contribution statement

David Latorre-Arca: Writing – review & editing, Writing – original draft, Investigation, Formal analysis. **M. Soledad Larrechi:** Writing – review & editing, Writing – original draft, Visualization, Validation, Supervision, Methodology, Investigation, Formal analysis, Conceptualization. **Daniel Salavera:** Supervision, Project administration, Investigation, Funding acquisition, Conceptualization. **Alberto Coronas:** Writing – review & editing, Supervision, Funding acquisition.

Declaration of competing interest

The authors declare that they have no known competing financial interests or personal relationships that could have appeared to influence the work reported in this paper.

Acknowledgements

The authors thank the Spanish Ministry of Science and Innovation for funding this project (PID2020-119004RB-C21). The authors acknowledge YTC America for support in measuring the properties of the

solutions with [Bmim][Br] and for granting permission to publish the results. David Latorre Arca also acknowledges the Diputació de Tarragona and the Universitat Rovira i Virgili for their financial support, and Cristina Segovia Martín for her help and participation in the experimental determination of the SLE.

Appendix A. Supplementary data

Supplementary data to this article can be found online at https://doi.org/10.1016/j.molliq.2025.127302.

Data availability

Data will be made available on request.

References

[1] R. Nikbakhti, X. Wang, A.K. Hussein, A. Iranmanesh, Absorption cooling systems – review of various techniques for energy performance enhancement, Alex. Eng. J. 59 (2020) 707–738, https://doi.org/10.1016/j.aej.2020.01.036.
[2] P. Srikhirin, S. Aphornratana, S. Chungpaibulpatana, A review of absorption refrigeration technologies, Renew. Sustain. Energy Rev. 5 (2001) 343–372, https://doi.org/10.1016/S1364-0321(01)00003-X.
[3] X. Wang, H.T. Chua, Absorption cooling: a review of lithium bromide-water chiller technologies, Recent Pat. Mech. Eng. 2 (2009) 193–213, https://doi.org/10.2174/1874477x10902030193.
[4] K.E. Herold, R. Radermacher, S.A. Klein. Absorption Chillers and Heat Pumps, second ed., CRC Press, 2016 https://doi.org/10.1201/b19625.
[5] D. Salavera Muñoz, Propiedades termofísicas de nuevos fluidos de trabajo (H2O+LiBr+LiNO3+LiCl+LiI, NH3+H2O+NaOH y NH3+H2O+KOH) para sistemas de refrigeración por absorción, 2005, Doctoral thesis, Universitat Rovira i Virgili, Tarragona, Spain. https://www.tdx.cat/handle/10803/8530.
[6] H.M. Ariyadi, Thermodynamic study on absorption refrigeration systems using ammonia/ionic liquid working pairs, Doctoral thesis, Universitat Rovira i Virgili, Tarragona, Spain, 2016. https://www.tdx.cat/handle/10803/396178.
[7] A. Cera-Manjarres, Experimental determination and modelling of thermophysical properties of ammonia/ionic liquid mixtures for absorption refrigeration systems, Doctoral thesis, Universitat Rovira i Virgili, Tarragona, Spain, 2015. https://tdx.cat/handle/10803/404017.
[8] R. Rives, A. Coronas, A preliminary analysis of the influence of mass diffusivity on the performance of ammonia/ionic liquids absorption refrigeration cycles, in: International Sorption Heat Pump Conference 2021 Proceedings, 2021, pp. 92–96, https://doi.org/10.14279/depositonce-12278.
[9] M.S. Larrechi, A. Cera-Manjarres, A. Coronas, Ranking the solubility of ammonia in ionic liquids using near infrared spectroscopy and multivariate curve resolution, Spectrochim. Acta A Mol. Biomol. Spectrosc. 215 (2019) 88–96, https://doi.org/10.1016/j.saa.2019.02.090.
[10] M.S. Larrechi, A. Cera-Manjarres, D. Salavera, A. Coronas, Quantitative analysis of the interaction of ammonia with 1-(2-hydroxyethyl)-3-methylimidazolium tetrafluoroborate ionic liquid. Understanding the volumetric and transport properties of their mixtures, J. Mol. Liq. 301 (2020), https://doi.org/10.1016/j.molliq.2020.112440.
[11] J. Prieto, D. Salavera, A. Coronas, Experimental evaluation of the water absorption process in a horizontal tube falling film absorber with aqueous solutions of [Emim][OAc] and different tube materials, in: International Sorption Heat Pump Conference 2021 Proceedings, 2021, pp. 88–91, https://doi.org/10.14279/depositonce-12278.
[12] Y. Guo, J. Cao, F. Wang, Y. Ding, J. Li, P. Paricaud, Experimental and modelling of the vapor-liquid equilibria of [Cnmim]Br(n = 2, 3, 4) + H2O systems, Fluid Phase Equilib. 565 (2023), https://doi.org/10.1016/j.fluid.2022.113654.
[13] A. Ayad, T. Di Pietro, F. Mutelet, A. Negadi, Thermodynamic properties of tricyanomethanide-based ionic liquids with water: experimental and modelling, J. Solution Chem. 50 (2021) 517–543, https://doi.org/10.1007/s10953-021-01072-9.
[14] M. Królikowska, M. Zawadzki, Physicochemical properties of tri(butyl) ethylphosphonium diethylphosphate aqueous mixtures, J. Mol. Liq. 249 (2018) 153–159, https://doi.org/10.1016/j.molliq.2017.11.011.
[15] A. Yokozeki, M.B. Shiflett, Water solubility in ionic liquids and application to absorption cycles, Ind. Eng. Chem. Res. 49 (2010) 9496–9503, https://doi.org/10.1021/ie1011432.
[16] Y. Guo, Y. Ding, J. Li, P. Paricaud, The performance of [Emim]Br/H2O as a working pair in the absorption refrigeration system, Next Energy 2 (2024) 100038, https://doi.org/10.1016/j.nxener.2023.100038.
[17] J. Sun, L. Fu, S. Zhang, A review of working fluids of absorption cycles, Renew. Sustain. Energy Rev. 16 (2012) 1899–1906, https://doi.org/10.1016/j.rser.2012.01.011.
[18] M. Khamooshi, K. Parham, U. Atikol, Overview of ionic liquids used as working fluids in absorption cycles, Adv. Mech. Eng. 5 (2013) 620592, https://doi.org/10.1155/2013/620592.
[19] D. Latorre-Arca, D. Salavera, M.S. Larrechi, A. Coronas, Influence of 1,3-dimethylimidazolium chloride on the solubility of lithium bromide in water for absorption refrigeration and heat pumps, in: Avances En Ciencias y Técnicas Del Frío - 11, Ediciones UPCT, 2022, pp. 156–160. doi: 10.31428/10317/11521.
[20] D. Latorre-Arca, D. Salavera, M.S. Larrechi, A. Coronas, Analysis of the chemical interactions and vapor pressure in H2O/(LiBr+1,3-dimethylimidazolium chloride) mixtures, in: Proceedings of the XII National and III International Conference on Engineering Thermodynamics, 2022, pp. 1195–1200. ISBN: 978-84-09-42477-1.
[21] M. Królikowska, M. Skonieczny, K. Paduszyński, Physicochemical and thermodynamic investigation of ethanolic solution of phosphonium-based ionic liquids—measurements, correlations, and application to absorption cycles, J. Chem. Eng. Data 68 (2023) 3377–3397, https://doi.org/10.1021/acs.jced.3c00537.
[22] L. Ji, S.K. Shukla, Z. Zuo, X. Lu, X. Ji, C. Wang, An overview of the progress of new working pairs in absorption heat pumps, Energy Rep. 9 (2023) 703–729, https://doi.org/10.1016/j.egyr.2022.11.143.
[23] D. Salavera, D. Latorre-Arca, H.A. Tariq, M.S. Larrechi, A. Coronas, Selección de un aditivo para H2O/LiBr en sistemas de refrigeración y bombas de calor por absorción en base a la determinación cuantitativa de la hidratación del LiBr, in: Libro de Resúmenes Del XII Congreso Ibérico y X Congreso Iberoamericano de Ciencias y Técnicas Del Frío CYTEF 2024, 2024. https://doi.org/10.21134/27022a20.
[24] H.A. Tariq, A. Altamirano, R. Collignon, B. Stutz, A. Coronas, Experimental study on the effect of an ionic liquid as anti-crystallization additive in a bi-adiabatic H2O-LiBr absorption chiller prototype, Appl. Therm. Eng. 259 (2025) 124756, https://doi.org/10.1016/j.applthermaleng.2024.124756.
[25] N.V. Plechkova, K.R. Seddon, Applications of ionic liquids in the chemical industry, Chem. Soc. Rev. 37 (2008) 123–150, https://doi.org/10.1039/b006677j.
[26] C. D'Agostino, M.D. Mantle, C.L. Mullan, C. Hardacre, L.F. Gladden, Diffusion, ion pairing and aggregation in 1-ethyl-3-methylimidazolium-based ionic liquids studied by 1H and 19F PFG NMR: effect of temperature, anion and glucose dissolution, ChemPhysChem 19 (2018) 1081–1088, https://doi.org/10.1002/cphc.201701354.
[27] K.S. Kim, D. Demberelnyamba, B.K. Shin, S.H. Yeon, S. Choi, J.H. Cha, H. Lee, C. S. Lee, J.J. Shim, Surface tension and viscosity of 1-butyl-3-methylimidazolium iodide and 1-butyl-3-methylimidazolium tetrafluoborate, and solubility of lithium bromide+1-butyl-3-methylimidazolium bromide in water, Korean J. Chem. Eng. 23 (2006) 113–116, https://doi.org/10.1007/BF02705701.
[28] M. Królikowska, T. Hofman, The influence of bromide-based ionic liquids on solubility of LiBr (1) + water (2) system. Experimental (solid + liquid) phase equilibrium data, Part 1, J Mol Liq 273 (2019) 606–614, https://doi.org/10.1016/j.molliq.2018.09.104.
[29] L. Jing, Z. Danxing, F. Lihua, W. Xianghong, D. Li, Vapor pressure measurement of the ternary systems H2O + LiBr + [Dmim]Cl, H2O + LiBr + [Dmim]BF4, H2O + LiCl + [Dmim]Cl, and H2O + LiCl + [Dmim]BF4, J. Chem. Eng. Data 56 (2011) 97–101, https://doi.org/10.1021/je1009202.
[30] M. Yizhak, Effect of ions on the structure of water: Structure making and breaking, Chem. Rev. 109 (2009) 1346–1370, https://doi.org/10.1021/cr8003828.
[31] M. Yizhak, G. Hefter, Ion pairing, Chem. Rev. 106 (2006) 4585–4621, https://doi.org/10.1021/cr040087x.
[32] M. Yizhak. Ions in Solution and Their Solvation, John Wiley & Sons, Inc, 2015, https://doi.org/10.1002/9781118892336.
[33] T. Méndez-Morales, J. Carrete, Ó. Cabeza, O. Russina, A. Triolo, L.J. Gallego, L. M. Varela, Solvation of lithium salts in protic ionic liquids: a molecular dynamics study, J. Phys. Chem. B 118 (2014) 761–770, https://doi.org/10.1021/jp410090f.
[34] P. Vallet, S. Bouzón-Capelo, T. Méndez-Morales, V. Gómez-González, Y. Arosa, R. de la Fuente, E. López-Lago, J.R. Rodríguez, L.J. Gallego, J.J. Parajó, J. Salgado, M. Turmine, L. Segade, O. Cabeza, L.M. Varela, On the physical properties of mixtures of nitrate salts and protic ionic liquids, J. Mol. Liq. 350 (2022), https://doi.org/10.1016/j.molliq.2022.118483.
[35] T. Méndez-Morales, J. Carrete, S. Bouzón-Capelo, M. Pérez-Rodríguez, Ó. Cabeza, L.J. Gallego, L.M. Varela, MD simulations of the formation of stable clusters in mixtures of alkaline salts and imidazolium-based ionic liquids, J. Phys. Chem. B 117 (2013) 3207–3220, https://doi.org/10.1021/jp312669r.
[36] T. Méndez-Morales, J. Carrete, Ó. Cabeza, L.J. Gallego, L.M. Varela, Molecular dynamics simulation of the structure and dynamics of water-1-alkyl-3-methylimidazolium ionic liquid mixtures, J. Phys. Chem. B 115 (2011) 6995–7008, https://doi.org/10.1021/jp202692g.
[37] J.M. Otero-Mato, V. Lesch, H. Montes-Campos, J. Smiatek, D. Diddens, O. Cabeza, L.J. Gallego, L.M. Varela, Solvation in ionic liquid-water mixtures: A computational study, J. Mol. Liq. 292 (2019), https://doi.org/10.1016/j.molliq.2019.111273.
[38] L. Segade, M. Cabanas, M. Domínguez-Pérez, E. Rilo, S. García-Garabal, M. Turmine, L.M. Varela, V. Gómez-González, B. Docampo-Alvarez, O. Cabeza, Surface and bulk characterisation of mixtures containing alkylammonium nitrates and water or ethanol: experimental and simulated properties at 298.15 K, J. Mol. Liq. 222 (2016) 663–670, https://doi.org/10.1016/j.molliq.2016.07.107.
[39] M.S. Rodríguez-Barrios, A. Rodríguez-Fortea, L.M. Varela, D. Salavera, M. S. Larrechi, A. Coronas, Structural and quantitative analysis of water association in ethylammonium nitrate mixtures using soft modeling resolution of NIR spectra and molecular dynamics simulations, J. Mol. Liq. 327 (2021) 114789, https://doi.org/10.1016/j.molliq.2020.114789.
[40] B. Docampo-Álvarez, V. Gómez-González, T. Méndez-Morales, J. Carrete, J. R. Rodríguez, Ó. Cabeza, L.J. Gallego, L.M. Varela, Mixtures of protic ionic liquids and molecular cosolvents: a molecular dynamics simulation, J. Chem. Phys. 140 (2014), https://doi.org/10.1063/1.4879660.
[41] A.A. Zavitsas, Ideal thermodynamic behaviors of aqueous electrolyte solutions at very high concentrations, Chem. Phys. Lett. 759 (2020) 137941, https://doi.org/10.1016/j.cplett.2020.137941.

[42] R. Heyrovská, Partial dissociation and hydration quantitatively explain the properties of aqueous electrolyte solutions and hence empirical activity concepts are unnecessary, Nature Prec. (2011), https://doi.org/10.1038/npre.2011.6416.1.
[43] J.G. Reynolds, T.R. Graham, C.I. Pearce, Extending Zavitsas' hydration model to the thermodynamics of solute mixtures in water, J. Mol. Liq. 347 (2022) 118309, https://doi.org/10.1016/j.molliq.2021.118309.
[44] A.D. Wilson, C. Stetson, Modeling solution vapor equilibria with solvation and solute assembly, J. Mol. Liq. 336 (2021) 116272, https://doi.org/10.1016/j.molliq.2021.116272.
[45] A.D. Wilson, H. Lee, C. Stetson, Mass action model of solution activity via speciation by solvation and ion pairing equilibria, Commun. Chem. 4 (2021) 163, https://doi.org/10.1038/s42004-021-00599-8.
[46] M.I. Barba, M.S. Larrechi, A. Coronas, Quantitative analysis of the hydration of lithium salts in water using multivariate curve resolution of near-infrared spectra, Anal. Chim. Acta 919 (2016) 20–27, https://doi.org/10.1016/j.aca.2016.03.022.
[47] M.I. Barba, M.S. Larrechi, A. Coronas, Quantitative analysis of free water in ionic liquid-water mixtures, Talanta 199 (2019) 407–414, https://doi.org/10.1016/j.talanta.2019.02.087.
[48] D. Latorre-Arca, M. Soledad Larrechi, D. Salavera, A. Coronas, A. Rodríguez-Fortea, A. Rivera-Pousa, T. Méndez-Morales, L.M. Varela, Quantitative and structural analysis of water association in water-lithium bromide-1,3-dimethylimidazolium chloride mixtures, J. Mol. Liq. 368 (2022) 120828, https://doi.org/10.1016/j.molliq.2022.120828.
[49] D. Latorre-Arca, Quantitative analysis of bulk water in water/lithium bromide mixtures with ionic liquids as a working fluid in absorption heat pumps and influence on the thermophysical properties, Doctoral thesis, Universitat Rovira i Virgili, Tarragona, Spain, 2024. https://www.tdx.cat/handle/10803/692789.
[50] D. Salavera, X. Esteve, K.R. Patil, A.M. Mainar, A. Coronas, Solubility, heat capacity, and density of lithium bromide + lithium iodide + lithium nitrate + lithium chloride aqueous solutions at several compositions and temperatures, J. Chem. Eng. Data 49 (2004) 613–619, https://doi.org/10.1021/je034202x.
[51] M. Królikowska, M. Zawadzki, M. Skonieczny, The influence of bromide-based ionic liquids on solubility of LiBr (1) + water (2) system. Experimental (solid + liquid) phase equilibrium data Part 2, J. Mol. Liq. 265 (2018) 316–326, https://doi.org/10.1016/j.molliq.2018.06.006.
[52] M. Królikowska, N. Świtalska, M. Zawadzki, The experimental study on the (solid + liquid) phase equilibria for LiBr (1) + ionic liquid (2) + water (3) systems, Fluid Phase Equilib. (2024) 114164, https://doi.org/10.1016/j.fluid.2024.114164.
[53] D. Yang, Y. Zhu, S. Liu, H. Lv, C. Luo, Thermodynamic properties of a ternary AHP working pair: lithium bromide + 1-ethyl-3-methylimidazolium chloride + H2O, J. Chem. Eng. Data 64 (2019) 574–583, https://doi.org/10.1021/acs.jced.8b00771.
[54] The MathWorks Inc. (2021). Matlab version: 9.10.0 (R2021a). Natick, Massachusetts: The MathWorks Inc. https://www.mathworks.com.
[55] R. Tauler, B. Kowalski, S. Fleming, Multivariate curve resolution applied to spectral data from multiple runs of an industrial process, Anal. Chem. 65 (1993) 2040–2047, https://doi.org/10.1021/ac00063a019.
[56] J. Jaumot, A. de Juan, R. Tauler, MCR-ALS GUI 2.0: New features and applications, Chemomet. Intell. Lab. Syst. 140 (2015) 1–12, https://doi.org/10.1016/j.chemolab.2014.10.003.
[57] M. Maeder, A.D. Zuberbuehler, The resolution of overlapping chromatographic peaks by evolving factor analysis, Anal. Chim. Acta 181 (1986) 287–291, https://doi.org/10.1016/S0003-2670(00)85248-4.
[58] R. Tauler, A. Izquierdo-Ridorsa, E. Casassas, Simultaneous analysis of several spectroscopic titrations with self-modelling curve resolution, Chemom. Intel. Lab. Syst. 18 (1993) 293–300, https://doi.org/10.1016/0169-7439(93)85006-3.
[59] J. Pátek, J. Klomfar, Solid-liquid phase equilibrium in the systems of LiBr-H2O and LiCl-H2O, Fluid Phase Equilib. 250 (2006) 138–149, https://doi.org/10.1016/j.fluid.2006.09.005.
[60] L. Kacenauskaite, S.J. Van Wyck, M. Moncada Cohen, M.D. Fayer, Water-in-salt: fast dynamics, structure, thermodynamics, and bulk properties, J. Phys. Chem. B 128 (2023) 291–302, https://doi.org/10.1021/acs.jpcb.3c07711.
[61] A.A. Chen, R.V. Pappu, Quantitative characterization of ion pairing and cluster formation in strong 1:1 electrolytes, J. Phys. Chem. B 111 (2007) 6469–6478, https://doi.org/10.1021/jp0708547.